Published in final edited form as:

Biochem J. 2023 September 27; 480(18): 1459–1473. doi:10.1042/BCJ20230075.

Lhs1 dependent ERAD is determined by transmembrane domain context

Maria Sukhoplyasova[1], **Abigail M. Keith**[1], **Emma M. Perrault**[1], **Hannah E. Vorndran**[1], **Alexa S. Jordahl**[1], **Megan E. Yates**[1], **Ashutosh Pastor**[1], **Zachary Li**[1], **Michael L. Freaney**[1], **Riddhi A. Deshpande**[1], **David B. Adams**[1], **Christopher J. Guerriero**[1], **Shujie Shi**[2], **Thomas R. Kleyman**[2,3,4], **Ossama B. Kashlan**[2], **Jeffrey L. Brodsky**[1], **Teresa M. Buck**[1]

[1]Department of Biological Sciences, University of Pittsburgh, Pittsburgh, PA, U.S.A.

[2]Renal-Electrolyte Division, Department of Medicine, University of Pittsburgh, Pittsburgh, PA, U.S.A.

[3]Department of Cell Biology, University of Pittsburgh, Pittsburgh, PA, U.S.A.

[4]Department of Pharmacology and Chemical Biology, University of Pittsburgh, Pittsburgh, PA, U.S.A.

Abstract

Transmembrane proteins have unique requirements to fold and integrate into the endoplasmic reticulum (ER) membrane. Most notably, transmembrane proteins must fold in three separate environments: extracellular domains fold in the oxidizing environment of the ER lumen, transmembrane domains (TMDs) fold within the lipid bilayer, and cytosolic domains fold in the reducing environment of the cytosol. Moreover, each region is acted upon by a unique set of chaperones and monitored by components of the ER associated quality control machinery that identify misfolded domains in each compartment. One factor is the ER lumenal Hsp70-like chaperone, Lhs1. Our previous work established that Lhs1 is required for the degradation of the unassembled α-subunit of the epithelial sodium channel (αENaC), but not the homologous β- and γENaC subunits. However, assembly of the ENaC heterotrimer blocked the Lhs1-dependent ER associated degradation (ERAD) of the α-subunit, yet the characteristics that dictate the specificity of Lhs1-dependent ERAD substrates remained unclear. We now report that Lhs1-dependent substrates share a unique set of features. First, all Lhs1 substrates appear to be unglycosylated,

Correspondence: Teresa M. Buck (teb20@pitt.edu).

CRediT Author Contribution

Teresa M. Buck: Conceptualization, Formal analysis, Supervision, Funding acquisition, Investigation, Writing — original draft, Writing — review and editing. **Maria Sukhoplyasova:** Investigation, Writing — review and editing. **Abigail M. Keith:** Investigation, Writing — review and editing. **Emma M. Perrault:** Investigation, Writing — review and editing. **Hannah E. Vorndran:** Investigation. **Alexa S. Jordahl:** Investigation, Writing — review and editing. **Megan E. Yates:** Investigation, Writing — review and editing. **Ashutosh Pastor:** Investigation, Writing — review and editing. **Zachary Li:** Investigation, Writing — review and editing. **Michael L. Freaney:** Investigation, Writing — review and editing. **Riddhi A. Deshpande:** Investigation, Writing — review and editing. **David B. Adams:** Investigation, Writing — review and editing. **Christopher Guerriero:** Conceptualization, Funding acquisition, Investigation, Writing — review and editing. **Shujie Shi:** Resources, Writing — review and editing. **Thomas R. Kleyman:** Conceptualization, Funding acquisition, Writing — review and editing. **Ossama Kashlan:** Investigation, Writing — review and editing. **Jeffrey L. Brodsky:** Conceptualization, Supervision, Writing — review and editing.

Competing Interests

The authors declare that there are no competing interests associated with the manuscript.

and second they contain two TMDs. Each substrate also contains orphaned or unassembled TMDs. Additionally, interfering with inter-subunit assembly of the ENaC trimer results in Lhs1-dependent degradation of the entire complex. Finally, our work suggests that Lhs1 is required for a subset of ERAD substrates that also require the Hrd1 ubiquitin ligase. Together, these data provide hints as to the identities of as-yet unconfirmed substrates of Lhs1 and potentially of the Lhs1 homolog in mammals, GRP170.

Introduction

The assembly of multi-spanning or multimeric transmembrane domain (TMD) containing proteins is complex, one that often results in the production of misfolded or misassembled proteins. Misfolded and misassembled proteins are recognized by the quality control machinery in the endoplasmic reticulum (ER) and targeted for degradation by the cytosolic 26S proteasome. This process is termed ERAD (endoplasmic reticulum associated degradation) [1–6].

Most misfolded proteins are recognized for ERAD by molecular chaperones in the ER lumen and cytosol, extracted or retrotranslocated into the cytosol, ubiquitinated by E3 ligases, and delivered to the proteasome. In yeast, the necessary flexibility required for ERAD substrate recognition with unique membrane topologies is facilitated by the aforementioned molecular chaperones as well as specific E3s, i.e. Hrd1 and Doa10 [7,8]. The Hrd1 complex most commonly recognizes folding lesions in the ER lumen or membrane (‘ERAD-L/M’), whereas the Doa10 complex recognizes cytosolic lesions (‘ERAD-C’) [9]. Although chaperone-based ‘decisions’ frequently depend on Hsp70, a poorly characterized molecular chaperone, Lhs1, is also required for the ERAD of select substrates [10]. The spectrum of Lhs1-dependent substrates — or substrates recognized by the homologous GRP170 chaperone in mammalian cells — is currently unclear.

Like canonical Hsp70s, Lhs1 contains three domains, an ATPase domain, a substrate binding domain, and a lid domain [11]. Unlike traditional Hsp70s, Lhs1 also contains a large unstructured loop within the substrate binding domain and an extended C-terminal α-helical region [12,13]. Early work established that Lhs1 functions in two distinct processes. First, Lhs1 acts as a nucleotide exchange factor (NEF) and co-chaperone for the ER lumenal Hsp70, Kar2/BiP, and mutations in Lhs1 inhibit the co-translational translocation of some secreted proteins [14–17]. In addition, deletion of both Lhs1 and the other ER lumenal NEF, Sil1, leads to a synthetic lethal phenotype in yeast [17]. Second, Lhs1 possesses BiP-independent ‘holdase’ activity: Lhs1 prevents the aggregation of a misfolded protein [18], and GRP170 binds preferentially to aggregation-prone regions in misfolded substrates [19,20]. The importance of GRP170 is underscored by the fact that the loss of GRP170 is embryonic lethal [17], and an inducible, nephron-specific GRP170 knock-out mouse model leads to rapid induction of the unfolded protein response (UPR), widespread kidney injury, and defects in salt and water homeostasis [21].

We previously determined that Lhs1/GRP170 is required for the ERAD of the α-subunit of the epithelial sodium channel, ENaC, a renal heterotrimeric sodium channel composed primarily of homologous α, β, and γ subunits (Figure 1A) [22–26]. In contrast, the loss

of Lhs1 had no effect on either β- or γENaC degradation [10]. All three ENaC subunits assemble in the ER prior to plasma membrane transport [27–29], and indeed co-expression of the β- and γENaC subunits with the α-subunit — and thus assembly of the ENaC TMDs — blocked Lhs1-targeted degradation of αENaC (Figure 1B) [30]. We also reported that a lower-molecular weight unglycosylated αENaC species accumulated in yeast lacking Lhs1, yet the higher molecular weight/mature glycosylated subunit was degraded. In accordance with these results, GRP170 overexpression in either *Xenopus* oocytes or mammalian cells destabilized αENaC, and GRP170 preferentially associated with unglycosylated αENaC [10]. Why TMD assembly blocks Lhs1-targeted degradation and other features that dictate Lhs1 specificity are unknown.

By surveying model ERAD substrates in yeast containing or lacking Lhs1, we now confirm that the TMDs of αENaC are a transferable signal for Lhs1-directed ERAD. We also find that interfering with predicted intermolecular interactions between the ENaC subunits not only blocks TMD interactions but leads to Lhs1-dependent degradation of the α-subunit, along with the β- and γ-subunit. Next, we show that Lhs1 targets dual-spanning TMD proteins for ERAD that contain orphaned or unassembled TMDs, and that degradation requires the Hrd1 ubiquitin ligase.

Results

Our previous work reported that loss of Lhs1 stabilized a lower-molecular weight unglycosylated αENaC species (see Figure 1A for a recent example) [10,30], but had no effect on the stability of the β- or γENaC subunits [30]. We also determined that the αENaC TMDs and oligomeric assembly with the TMDs of the other subunits regulate Lhs1-mediated degradation [30]. Inter-subunit assembly of the ENaC TMDs blocks Lhs1-targeted ERAD (Figure 1B, and as previously shown [30]). However, the mechanism by which the TMDs are recognized is unknown, as are the more general properties that dictate Lhs1 substrate specificity.

Lhs1 dependence is transferable between ENaC subunits

To determine if the signal for Lhs1 dependence is transferable — and thus represents an Lhs1-dependent degron — we inserted the TMDs from αENaC into βENaC ($\beta ENaC_{\alpha TM1–2}$) and reciprocally replaced the αENaC TMDs with those from βENaC ($\alpha ENaC_{\beta TM1–2}$) (Figure 1C). We expressed these constructs in *LHS1* and *Δlhs1* yeast and performed cycloheximide chases to determine protein stability. As shown in Figure 1C, top panels, insertion of the αENaC TMDs into βENaC stabilized a lower-molecular weight, unglycsoylated species, and likewise inserting the βENaC TMDs into αENaC resulted in a more βENaC-like profile (bottom panels). Notably, the stable, unglycosylated species — a hallmark of Lhs1-dependent ERAD — is no longer present. These results support the notion that the αENaC TMDs are both an essential and transferrable motif for Lhs1-assisted degradation.

To assess how the TMDs of αENaC vary from those of β- and γENaC, we analyzed the relative apparent free energies for membrane insertion (ΔG_{app}) of each TMD using dgpred (https://dgpred.cbr.su.se/index.php?p=TMpred) [30]. While the ΔG_{app} for the second

TMD of all three ENaC subunits is similar (+4.3 to +5.9), the predicted ΔG_{app} for αENaC TMD1 is far less favorable than TMD1 from either β- or γENaC (+0.24 vs −2.4 and −3.3). Because prior work showed that membrane instability favors ERAD [31], we hypothesized that making the ΔG_{app} for membrane insertion of the αENaC TMD1 more favorable would decrease Lhs1-dependence. Therefore, two mutations in αENaC TMD1, E133A/E134A, were constructed to increase hydrophobicity and reduce the predicted ΔG_{app} from +0.24 to −2.1 kcal/mol (Figure 1D). Contrary to our prediction, these mutations further destabilized αENaC in WT yeast (Figure 1E and compare to Figure 1C; note the absence of protein at the 30 min time point).

Hydrophobic mutations in αENaC TMD1 may interfere with stabilizing inter-subunit contacts

When the β- and γENaC subunits are co-expressed with αENaC, channel assembly completely blocks Lhs1-dependent ERAD of the α-subunit (see Figure 1B and [30]). However, when we co-expressed the β- and γENaC subunits with $\alpha ENaC_{E132A/E133A}$ in *WT* or *Δlhs1* yeast strains, the stable lower-molecular weight species remained in the *Δlhs1* strain (Figure 2A). Unlike WT αENaC, the degradation of $\alpha ENaC_{E132A/E133A}$ was unaffected by co-expression of βγENaC. Because these data suggest a defect in ENaC TMD interactions, we used a structural model [32] of the TMDs and identified a predicted polar interaction between αENaC E133 and βENaC N512 (Figure 2B). Therefore, we examined whether the single hydrophobic E133A mutation might disrupt inter-subunit TMD interactions and alter Lhs1-dependence. Consistent with our hypothesis, a single alanine substitution in αENaC TMD1(E133A) led to the presence of the stable, lower-molecular weight αENaC species in the *Δlhs1* mutant when co-expressed with β and γENaC (Figure 2C, top panels, and quantified time-course data in Supplementary Figure S2B), consistent with defects in functional TMD interactions. Surprisingly, in the context of the $\alpha ENaC_{E133A}$ mutant, the degradation profiles of both β- and γENaC were also altered in the *Δlhs1* strain. In contrast, when expressed individually, the loss of Lhs1 affected neither β nor γENaC [10]. We confirmed that the degradation of $\alpha ENaC_{E133A}$ expressed alone was stabilized in the *Δlhs1* strain, as expected (Supplementary Figure S2A). We therefore suggest that subtle perturbations between the α and βENaC TMDs lead to Lhs1-dependent degradation of the entire channel (also see Discussion).

Disrupting putative polar intermolecular interactions between the ENaC TMDs targets β- and γENaC for Lhs1-dependent ERAD

Based on the results presented above, we asked if disrupting putative polar contacts between the ENaC TMDs generally impairs inter-subunit TMD assembly and promotes Lhs1-dependent degradation of all three ENaC subunits. To answer this question, we first generated the N512A mutation in TMD2 of βENaC, which we predicted would interact with αENaC E133 (Figure 2B). Consistent with our hypothesis, the βN512A mutant failed to block the Lhs1-dependent ERAD of αENaC (Figure 3A and quantified time-course data in Supplementary Figure S2C). In other words, disrupting the polar inter-subunit interaction, E133:βN512, shifts the β and γENaC subunits to what was previously seen as an αENaC-specific, Lhs1-dependent degradation pathway.

To determine if this effect is specific to αβENaC interactions, we then generated an alanine substitution to disrupt the second inter-subunit polar interaction that we propose exists between αS576 and γN536 (Figure 2B). We then performed cycloheximide chases in the context of $\alpha_{S576A}\beta\gamma$, as shown in Figure 3B (also see quantified time-course data in Supplementary Figure S2D). Interfering with the α_{S576A}:γ_{N536} polar interaction most likely compromised WT TMD interactions, as seen from the αENaC degradation profile, and resulted in a more αENaC-like degradation pathway for all three ENaC subunits. This was typified by the presence of a more stable, non-glycosylated ENaC species (−g). Therefore, if assembly of the ENaC pore-lining TMDs is disrupted, the βγENaC subunits are 'pulled' into the αENaC-like degradation pathway.

The degradation of ion channels and transporters containing additional TMDs is Lhs1-independent

To more generally define the properties that define Lhs1-directed degradation, we measured the ERAD of other ion channels as well as ion transporters expressed in *LHS1* and *Δlhs1* yeast (Figure 4A). We previously showed that the degradation rates of a 12 TMD Cl^- channel, the cystic fibrosis transmembrane conductance regulator (CFTR), and the soluble model ERAD substrate, CPY*, were unaffected by the loss of Lhs1 [10]. Here, the degradation of three ion channels targeted for ERAD in yeast, ROMK (renal outer medullary potassium channel), NCC (sodium chloride cotransporter), and ASIC1 (acid sensing ion channel) were measured. ASIC1 is an ENaC family member and is similarly a dual-spanning protein, but unlike ENaC, the subunit homotrimerizes. Surprisingly, ASIC1 degradation was unaffected in yeast lacking Lhs1 (Supplementary Figure S3A). The degradation of ROMK, a two TMD protein with a large cytosolic domain that tetramerizes, and NCC, a 12 TMD-containing protein, were also unaffected when the gene encoding Lhs1 was deleted (Supplementary Figure S3B,C). These results strongly suggest that the unassembled TMDs of αENaC, when expressed in the absence of βγENaC, represent a key feature that targets this protein for Lhs1-directed ERAD.

Dual-spanning ERAD substrates with unassembled TMDs are also targeted for Lhs1-depenent ERAD

Prior work established that a dual-spanning TMD substrate, Chimera A* (Figure 4A) [33], requires a cohort of cytosolic chaperones to ubiquitinate and maintain substrate solubility during ERAD [34]. Chimera A* contains the first TMD from the 12 TMD spanning ERAD substrate, Ste6* [35], along with a synthetic second TMD, both of which are fused to the truncated second nucleotide-binding domain (NBD2) of Ste6* (Figure 4A). The truncated NBD2, NBD2*, is a well-characterized degron that leads to recognition by the ERAD machinery and subsequent proteasome-dependent degradation [35]. Because Ste6 assembly is predicted to require multiple interactions between the 12 TMDs — based on the structures of related proteins [36] — we hypothesize that Chimera A*, like αENaC, would possess unassembled TMDs and become an Lhs1-dependent substrate. As anticipated, the loss of Lhs1 stabilized Chimera A* (Figure 4B), whereas degradation of Ste6*, even though it harbors a degron, was unaffected in the *Δlhs1* strain (Supplementary Figure S3D). Moreover, the degradation of Chimera A, which harbors the same TMDs as Chimera A* but lacks the degron, was also significantly slowed in the absence of Lhs1 (Figure 4C). We then tested

a third construct, TM-Ubc9^{ts}, in which the truncated NBD2 is replaced with a temperature-sensitive version of Ubc9 that acts as a cytosolic degron at elevated temperatures [33]. Consistent with the results in Figure 4B,C, TM-Ubc9^{ts} was Lhs1-dependent (Figure 4D).

As noted above, Chimera A* contains the first TMD from Ste6* along with a synthetic second TMD to ensure proper membrane insertion [34]. However, if the second TMD contains the bona fide second TMD from Ste6*, the majority of the protein exists as a single-spanning glycosylated species, known as Chimera N* (Figure 4A) [34]. When we examined Chimera N* degradation, only the dual spanning, unglycosylated Chimera N* species was Lhs1-dependent (Figure 4E; note that the glycosylation state of each substrate was confirmed by analysis with EndoH (Figure 4F) and quantification for the stability of unglycosylated and glycosylated species is shown in Supplementary Figure S4A).

Thus far, the Lhs1-dependent substrates we identified possess several common features. First, the substrates are dual spanning. Second, Lhs1-targeted substrates are unglycosylated. Third, all substrates contain TMDs that are either unassembled or in an orphaned state (i.e. αENaC, but not ASIC1). To further support these rules, we examined Sec62, a native two TMD protein that functions as a component of the Sec61 translocation machinery in yeast [37]. When the cytosolic degron, Deg1, is attached to the N-terminus of Sec62, Deg1–Sec62 is an ERAD substrate [38–41] (Figure 5A, model 1). Addition of Deg1 results in recognition by the ERAD-C machinery, yet surprisingly the majority of Deg1–Sec62 is glycosylated. Because the only N-linked glycosylation consensus sites in Deg1–Sec62 are predicted to reside in the cytosol and therefore should be inaccessible to the ER lumenal oligosaccharyltransferase machinery [41], two alternate topologies were proposed for Deg1–Sec62 (model 2 and 3) to account for substrate glycosylation.

For the following reasons, we hypothesized that none of the proposed topologically distinct conformers in Figure 5A would be Lhs1-dependent substrates. The protein in model 1 contains two native TMDs, and the proteins in model 2 and model 3 are glycosylated. Consistent with these predictions, the degradation rate of Deg1–Sec62 was unaffected by loss of Lhs1 (Figure 5B) [41]. In addition, because the Lhs1-dependent substrates we identified are unglycosylated, we also tested a Deg1–Sec61 N90D/N153D mutant in which the consensus sites for glycosylation are mutated [41]. Consistent with our hypothesis, the degradation of Deg1–Sec61 N90D/N153D remained Lhs1-independent (Figure 5C; the absence or presence of glycans was confirmed by EndoH digestion in Figure 5D). These data are consistent with Lhs1 targeting dual spanning, unglycosylated substrates with orphaned TMDs.

Lhs1 partners with the Hrd1 degradation complex to promote αENaC degradation

As discussed earlier, ERAD-M/L substrates require the E3 ligase, Hrd1, whereas ERAD-C substrates require, Doa10 [7–9]. It is unknown whether Lhs1-dependent substrates are targeted for ERAD-L/M and/or ERAD-C. Lhs1 was proposed to acts as a BiP co-chaperone to maintain the association between Deg1–Sec62 with an ER membrane complex that includes Hrd1 and the translocon components Sec61 and Sec62. Interestingly, any mutation that interferes with Hrd1/Sec62/Sec61 complex association, such as the loss of Lhs1 or mutations in either Sec61 or Sec62, shifts Deg1–Sec62 from a Hrd1 to Doa10 dependent

ERAD substrate [41]. Moreover, we previously determined that αENaC was stabilized in the absence of either Hrd1 or Doa10 [42].

To generalize the relationship between Lhs1 and the Hrd1/Sec61/Sec62 complex, we assayed αENaC degradation in *WT* and *Δlhs1* yeast strains in the absence of either Hrd1 or Doa10 (Figure 6A). Interestingly, eliminating both Hrd1 and Lhs1 resulted in a similar phenotype as the loss of Lhs1 alone, as shown by the stable lower-molecular weight species (Figure 6A, −g). In contrast, in *Δlhs1Δdoa10* yeast, there was preferential stabilization of the higher molecular weight, glycosylated species (+g) (see Supplementary Figure S5A for quantitation of each ENaC species in chase assays). These results suggest that Lhs1 helps target unglycosylated αENaC to the Hrd1 pathway, whereas Doa10 preferentially targets the glycosylated protein for degradation. Indeed, an αENaC species that lacks N-linked glycosylation sites (*Δ*GαENaC) [10] was preferentially stabilized in *Δhrd1*, but not *Δdoa10*, yeast strains (Figure 6B and Supplementary Figure S5B). Similar to results in an *Δlhs1* strain [10], loss of Hrd1 seems to result in the accumulation of more ubiquitinated *ΔG*αENaC rather than less modified protein (Supplementary Figure S5C), suggesting Hrd1 may be required for protein retrotranslocation. Of note, deletion of the E3s, especially loss of Hrd1, resulted in a laddering of higher molecular weight bands. We confirmed that these bands were insensitive to EndoH and thus likely represented O-linked glycans (Figure 6C). Indeed, as the residence time of misfolded proteins in the ER increases, substrate O-linked mannosylation can also occur [43].

We next tested the role of another member of the suggested Hrd1–Sec61–Sec62 complex, Sec61. Since the *SEC61* gene is essential, we expressed αENaC in *WT* yeast or *sec61–2*, a temperature-sensitive mutant strain [44]. Consistent with a role in degrading the unglycoslated species in conjunction with Lhs1, we again observed a stable, lower-molecular weight species of αENaC in the *sec61–2* strain (Figure 6D and a quantification of replicate time-courses in Supplementary Figure S5D), and the N-linked glycosylation status of the substrate was again confirmed by EndoH digestion (Figure 6E). Because Sec61 is also required for protein translocation, we then used carbonate extraction to confirm that the unglycosylated αENaC species was membrane integrated in the mutant strain. Similar to the control, i.e. native Sec61, both the glycosylated and unglycosylated species of αENaC remained in the pellet after treatment with alkaline buffer, whereas the soluble ER lumenal protein, PDI, shifted to the supernatant fraction (Figure 6F). Together, our results are consistent with a model that Hrd1 and Sec61 are partners with Lhs1 and help direct Lhs1-dependent unglycosylated substrates for ERAD.

Discussion

Our goal was to better define the function of Lhs1, a poorly characterized ER lumenal molecular chaperone, during ERAD. We determined that TMD characteristics and inter-domain contacts dictate whether Lhs1 is required for the selection of a given substrate for ERAD. We also demonstrated that Lhs1 dependence is transferable. Furthermore, we employed a series of well-characterized natural and/or model ERAD substrates to define which properties are common to Lhs1-dependent substrates (see Supplementary Table S1). Together, the loss of Lhs1 exclusively stabilizes unglycosylated, dual-spanning membrane

proteins, and in every case the substrate contains TMDs that are either unassembled members of a complex (e.g. αENaC) or harbor orphaned or non-native TMDs (e.g. the Chimera A* series; Figure 4A; also see Supplementary Table S3 for a summary of our results).

Other characteristics appear to be dispensable for Lhs1 based selection. For example, the bulk of ENaC is deposited in the ER lumen, which is where Lhs1 resides, but the largest domains in the Chimera A* series are cytosolic [34]. Yet, not all ENaC species undergo Lhs1-dependent degradation, and degradation of the single membrane-spanning Chimera A* derivative, Chimera N*, was also Lhs1-independent. In mammalian cells, three soluble proteins, the NHK variant of α−1-antitrypsin, Akita proinsulin, and a transthyretin mutant (D18G), as well as one single spanning protein, require the mammalian homolog of Lhs1, GRP170, for efficient degradation [45,46]. For NHK and transthyretin, GRP170 may act as a co-chaperone for BiP, but GRP170 prevented the aggregation of Akita proinsulin in the absence of BiP, which triggered degradation of Akita via the ER-phagy pathway. In the future, it will be vital to elaborate the repertoire of examined ERAD substrates in yeast and mammals to established if species-specific differences in substrate selection are evident, or whether other features dictate a reliance on Lhs1. In addition, as discussed above, ERAD substrates in yeast can be loosely categorized by their topology and location of the folding lesion. Yet, the rules do not appear to be followed as closely in mammalian cells [42,47]. This might also be reflected in the altered reliance on Lhs1 in these systems.

Soluble and integral membrane ERAD substrates require unique factors. For example, a yeast Derlin-like protein, the pseudo-rhomboid protease, Dfm1, is required for the retrotranslocation and ERAD of multi-spanning ERAD substrates. Interestingly, both Hrd1 (Pdr5*, Hmg2) and Doa10 (Ste6*) dependent substrates also require Dfm1 for retrotranslocation and efficient degradation [48]. Soluble (CPY* and KHN) and single spanning (KWW) substrates are instead Dfm1-independent but stabilized in the absence of another Derlin-like protein, Der1. Therefore, topology determines selection by Dfm1 and Der1 [48]. In another example, a transmembrane protein, TMUB1, facilitates the degradation of membrane proteins based on the relative hydrophobicity of the TMDs [49].

We also report that proper assembly of TMDs within the lipid bilayer prevents Lhs1-targeted degradation. We previously determined that mutations in ENaC that interfere with TMD assembly do not block all subunit–subunit interactions, and ENaC subunits with TMD swaps still co-immunoprecipitate with WT subunits [30]. This inter-subunit association is likely maintained by the large ENaC extracellular domains, which is supported by recent structural determinations of ENaC using cryo-EM [50]. In the future, it will be vital to use more refined methods to confirm that the disruption of, for example, polar contacts between inter-subunit TMDs subtly alters the structure of the trimeric channel.

We predict that point mutations that interfere with TMD assembly (αE133A, βN512A, αS576A) do not block inter-subunit interactions between the large ENaC extracellular domains but are TMD specific. Disrupting these polar, inter-subunit TMD interactions results in conversion of the entire heterotrimer to an Lhs1-dependent substrate; when either β- or γENaC are expressed as monomers, neither subunit is affected by the loss of Lhs1. In

essence, αENaC 'pulls' β- and γENaC into an Lhs1-dependent ERAD pathway. There are other examples of unassembled subunits of multimeric complexes being targeted for ERAD, such as the α-subunit of the Na^+/K^+ ATPase and the H^+, K^+-ATPase [51–54]. Additionally, dominant negative mutations of channels and transporters have been identified that interfere with the trafficking of the WT subunits (e.g. voltage gated Na^+ channel, KCNQ1, HERG channels, Kir2.1, and Ca^{2+} channels); reviewed in [55]). In these cases, a mutant subunit interferes with the assembly of a complex, resulting in ER retention and in many cases degradation of the entire complex. However, to our knowledge, our data represent the first example in which improper complex assembly results in an alternative degradation pathway for all associated members of the complex.

Each Lhs1-dependent substrate in this study lacks N-linked glycans. The oligosaccharyltransferase (OST) enzyme complex adds N-linked glycosylation cotranslationally as a protein emerges from the Sec61 translocon [56]. We use the presence of a stable lower-molecular weight species (i.e. the unglycosylated species) as a signature for Lhs1-dependent ERAD, but the lack of glycans is insufficient for Lhs1 dependence: glycanless versions of β- and γENaC are not Lhs1 substrates [10]. Previous work by our group and others showed that ENaC subunit glycosylation is inefficient in many systems [10,57,58]. Surprisingly, unglycosylated ENaC subunits still assemble and traffic to the cell surface [22,26], yet glycosylation of βENaC facilitates optimal channel trafficking [59]. Notably, only the unglycoslated species of Chimera N* was stabilized in the *Δlhs1* strain, even though the unglycosylated form is only a small percentage of total protein in WT yeast. We hypothesize that the glycosylated ENaC species do not require Lhs1 because they subject to an alternative ERAD pathway; e.g. ER lectins can recognize N-linked glycans and assist in both protein folding and degradation [60] but some ungycosylated proteins are recognized directly by the ER lumenal Hsp70, BiP [61].

We determined that ubiquitinated αENaC amassed at the ER membrane when Lhs1 was absent [30], suggesting that Lhs1 acts during retrotranslocation. These data are consistent with the evidence presented before and here that Lhs1 works in concert with Hrd1 and Sec61, both of which assist with retrotranslocation to remove ERAD substrates from the ER [39,62–69]. Interestingly, previous studies in mammalian cells found that GRP170 binds to a Hrd1 partner, Sel1, thus linking BiP to the Hrd1 complex [45].

In conclusion, we have refined the view of how a cohort of substrates is targeted for ERAD and advanced our understanding of how multi-subunit TMD complexes are recognized by the ER quality control machinery. In addition, we have advanced our understanding of ENaC channel TMD assembly and quality control. Gain of function mutations in ENaC lead to Liddle's syndrome and high blood pressure and hypoaldosteronism, whereas loss of function mutations result in low blood pressure/salt wasting [70,71]. ENaC activity is also a negative contributor in cystic fibrosis and is therefore being actively pursued as a drug target. Looking forward, it will be vital to test how Lhs1 acts on mutant and polymorphic forms of the ENaC subunits, as these data will further our understanding of ENaC quality control and trafficking and may lead to new insights into novel therapeutics.

Materials and methods

Yeast strains and growth conditions

Yeast strains were grown using standard conditions and protocols for media preparation at 26°C unless otherwise noted [72]. *BY4742* (*WT*) and *Δlhs1* strains were obtained from Open Biosystems (Thermo Scientific). *MHY500, Δlhs1, Δhrd1, Δdoa10, Δhrd1Δdoa10, Δhrd1Δlhs1*, and *Δdoa10Δlhs1* were generously provided by the Hochstrasser (Yale School of Medicine, New Haven, CT) or the Rubenstein (Ball State University, Muncie, IN) labs [41]. See Supplementary Table S2 for a complete list of yeast strains and sources.

Plasmid construction and molecular techniques

See Supplementary Table S3 for a complete list of plasmids and sources. Plasmids generated for this study: pRS423*GPD*-αENaC$_{E132A/E133A}$-HA, pRS423*GPD*-αENaC$_{E133A}$-HA, pRS426*GPD*-βENaCN$_{512A}$-13myc and pRS423*GPD*-αENaC$_{S576A}$ were generated using standard site directed mutagenesis protocols. All ENaC plasmids express murine ENaCs. ASIC1 was amplified from an expression vector (a gift from the Carattino Lab, University of Pittsburgh) and subcloned into the pRS415*TEF* expression vector [73] to generate pRS415*TEF* ASIC1(C70L)-HA.

Protein degradation assays

Cycloheximide chases were performed as previously described [42] unless otherwise noted in the text. Briefly, yeast transformed with the appropriate plasmid were grown overnight in selective media at 26°C. Cycloheximide at a final concentration of 50 μg/ml was added at time 0 and yeast were placed in a 37°C water bath. Samples were taken at the indicated times, and the yeast were pelleted and snap frozen in liquid N_2. Protein lysates were made from frozen pellets by alkaline lysis and TCA precipitation as previously described [42,74]. Precipitated protein pellets were resuspended in 80 ml TCA sample buffer (0.325 M Tris, pH 6.8, 10% SDS, 5% β-mercaptoethanol, and 0.25 mg/ml bromophenol blue) with a mechanical pestle grinder and immediately resolved by SDS–PAGE prior to western blot analysis.

Western blots were probed with the following antibodies as indicated in the text: anti-HA-HRP (clone 3F10; Roche Applied Science), anti-myc antiserum (Clontech), anti-V5 antibody (Novex), anti-FLAG (Cell signaling), anti-glucose-6-phosphate dehydrogenase antiserum (G6P; Sigma). The anti-myc, anti-V5 primary antibodies were then detected with anti-mouse monoclonal IgG HRP conjugated secondary antibody (Cell Signaling Technology). The anti-G6P and anti-FlAG primary antibodies were detected with a donkey horseradish peroxidase conjugated anti-rabbit IgG secondary antibody (GE Healthcare).

Other biochemical assays

For endoglycosidase H (endoH) digestion, the pH of protein lysates in SDS–PAGE sample buffer was adjusted with pH 9.5 Tris–HCl. Digestion was completed according to manufacturer's (Sigma) instructions for 2 hr at 37°C.

For carbonate extraction, yeast strains were transformed with the appropriate expression vector and grown overnight in selective media. A total of 50 ml of yeast at OD_{600} = 1.5 was harvested by centrifugation and resuspended in IP buffer (20 mM HEPES, pH = 7.4, 50 mM KOAc, 2 mM EDTA, 0.1 M Sorbitol, 1 mM DTT, 1 mM pepstatin A, 2 μg/ml, leupeptin, 1 mM PMSF and one protease inhibitor tablet (Roche)). Cells were disrupted with small glass beads and agitation on a vortex mixer for 4 × 1 min. Unbroken cells and cellular debris were removed by a slow-speed centrifugation (2500***g*** for 3 min). The supernatant was moved to a clean tube and centrifuged for 14 000g for 10 min at 4°C. Membrane pellets were resuspended in 500 μl IP butter and centrifuged at 14 000***g*** for 10 min at 4°C. The membranes were then resuspended in 100 μl Buffer 88 (20 mM HEPES, pH 6.8, 5 mM MgOAC, 150 mM KOAC, and 250 mM sorbitol)) + protease inhibitors, as above. A total of 40 μl of each sample was placed in a centrifuge tube and either 1 ml of 0.1 M Na_2CO_3 or Buffer 88 was added. Samples were incubated for 30 min on ice and then centrifuged for 50,000***g*** for 1 hr at 4°C. The supernatant was removed and saved, and the membrane pellet was resuspended in 500 ml of the appropriate buffer (carbonate or Buffer 88). Samples were then centrifuged at 60 000***g*** for 10 min. The supernatant was discarded, and the pellets were resuspended in 35 μl SDS–PAGE sample buffer with a mechanical pestle. A total of 100 μl of 50% TCA was added to each of the saved supernatant fractions and incubated on ice for 15 min followed by centrifugation at 14 000***g*** for 10 min at 4°C. The supernatant was aspirated, and pellets were resuspended in 35 μl of SDS–PAGE buffer using a mechanical pestle. All samples were incubated at 37°C for 10 min and then subject to SDS–PAGE and immunoblotting.

Supplementary Material

Refer to Web version on PubMed Central for supplementary material.

Acknowledgements

We would like to thank the members of the Brodsky lab and Linda Hendershot for input and scientific discussions. We also offer special thanks to Dr. Allyson O'Donnell for her thoughtful suggestions and critical analysis of this work for the entirety of the project, and the Rubenstein, Hochstrasser, and Carattino Labs for their generosity with reagents.

Funding

This work was supported by National Institutes of Health grants DK117162 (to T.M.B.), GM131732 (to J.L.B.), DK130901 (to S.S.), DK125439 (to O.B.K.), DK101584 (to C.J.G.), DK124659 (to C.J.G.), HL147818 (to T.R.K.) and DK079307 (Pittsburgh Center for Kidney Research).

Data Availability

All datasets for the study are available from the author upon request.

Abbreviations

CFTR	cystic fibrosis transmembrane conductance regulator
ER	endoplasmic reticulum

ERAD	ER associated degradation
NBD2	nucleotide-binding domain
NEF	nucleotide exchange factor
TMD	transmembrane domain
UPR	unfolded protein response

References

1. Kumari D. and Brodsky JL (2021) The targeting of native proteins to the endoplasmic reticulum-associated degradation (ERAD) pathway: an expanding repertoire of regulated substrates. Biomolecules 11, 1185 10.3390/biom11081185 [PubMed: 34439852]
2. Sun Z. and Brodsky JL (2019) Protein quality control in the secretory pathway. J. Cell Biol 218, 3171–3187 10.1083/jcb.201906047 [PubMed: 31537714]
3. Mehrtash AB and Hochstrasser M. (2019) Ubiquitin-dependent protein degradation at the endoplasmic reticulum and nuclear envelope. Semin. Cell Dev. Biol 93, 111–124 10.1016/j.semcdb.2018.09.013 [PubMed: 30278225]
4. Qi L, Tsai B. and Arvan P. (2017) New insights into the physiological role of endoplasmic reticulum-associated degradation. Trends Cell Biol. 27, 430–440 10.1016/j.tcb.2016.12.002 [PubMed: 28131647]
5. Wu X. and Rapoport TA (2018) Mechanistic insights into ER-associated protein degradation. Curr. Opin. Cell Biol 53, 22–28 10.1016/j.ceb.2018.04.004 [PubMed: 29719269]
6. Ruggiano A, Foresti O. and Carvalho P. (2014) Quality control: ER-associated degradation: protein quality control and beyond. J. Cell Biol 204, 869–879 10.1083/jcb.201312042 [PubMed: 24637321]
7. Denic V, Quan EM and Weissman JS (2006) A luminal surveillance complex that selects misfolded glycoproteins for ER-associated degradation. Cell 126, 349–359 10.1016/j.cell.2006.05.045 [PubMed: 16873065]
8. Carvalho P, Goder V. and Rapoport TA (2006) Distinct ubiquitin-ligase complexes define convergent pathways for the degradation of ER proteins. Cell 126, 361–373 10.1016/j.cell.2006.05.043 [PubMed: 16873066]
9. Vashist S. and Ng DT (2004) Misfolded proteins are sorted by a sequential checkpoint mechanism of ER quality control. J. Cell Biol 165, 41–52 10.1083/jcb.200309132 [PubMed: 15078901]
10. Buck TM, Plavchak L, Roy A, Donnelly BF, Kashlan OB, Kleyman TR et al. (2013) The Lhs1/GRP170 chaperones facilitate the endoplasmic reticulum-associated degradation of the epithelial sodium channel. J. Biol. Chem 288, 18366–18380 10.1074/jbc.M113.469882 [PubMed: 23645669]
11. Mayer MP and Bukau B. (2005) Hsp70 chaperones: cellular functions and molecular mechanism. Cell. Mol. Life Sci 62, 670–684 10.1007/s00018-004-4464-6 [PubMed: 15770419]
12. Shaner L. and Morano KA (2007) All in the family: atypical Hsp70 chaperones are conserved modulators of Hsp70 activity. Cell Stress Chaperones 12, 1–8 10.1379/CSC-245R.1 [PubMed: 17441502]
13. Behnke J, Feige MJ and Hendershot LM (2015) Bip and its nucleotide exchange factors Grp170 and Sil1: mechanisms of action and biological functions. J. Mol. Biol 427, 1589–1608 10.1016/j.jmb.2015.02.011 [PubMed: 25698114]
14. Baxter BK, James P, Evans T. and Craig EA (1996) SSI1 encodes a novel Hsp70 of the Saccharomyces cerevisiae endoplasmic reticulum. Mol. Cell. Biol 16, 6444–6456 10.1128/MCB.16.11.6444 [PubMed: 8887673]
15. Craven RA, Egerton M. and Stirling CJ (1996) A novel Hsp70 of the yeast ER lumen is required for the efficient translocation of a number of protein precursors. EMBO J. 15, 2640–2650 10.1002/j.1460-2075.1996.tb00624.x [PubMed: 8654361]

16. Steel GJ, Fullerton DM, Tyson JR and Stirling CJ (2004) Coordinated activation of Hsp70 chaperones. Science 303, 98–101 10.1126/science.1092287 [PubMed: 14704430]
17. Tyson JR and Stirling CJ (2000) LHS1 and SIL1 provide a lumenal function that is essential for protein translocation into the endoplasmic reticulum. EMBO J. 19, 6440–6452 10.1093/emboj/19.23.6440 [PubMed: 11101517]
18. de Keyzer J, Steel GJ, Hale SJ, Humphries D. and Stirling CJ (2009) Nucleotide binding by Lhs1p is essential for its nucleotide exchange activity and for function in vivo. J. Biol. Chem 284, 31564–31571 10.1074/jbc.M109.055160 [PubMed: 19759005]
19. Behnke J. and Hendershot LM (2014) The large Hsp70 Grp170 binds to unfolded protein substrates in vivo with a regulation distinct from conventional Hsp70s. J. Biol. Chem 289, 2899–2907 10.1074/jbc.M113.507491 [PubMed: 24327659]
20. Behnke J, Mann MJ, Scruggs FL, Feige MJ and Hendershot LM (2016) Members of the Hsp70 family recognize distinct types of sequences to execute er quality control. Mol. Cell 63, 739–752 10.1016/j.molcel.2016.07.012 [PubMed: 27546788]
21. Porter AW, Nguyen DN, Clayton DR, Ruiz WG, Mutchler SM, Ray EC et al. (2022) The molecular chaperone GRP170 protects against ER stress and acute kidney injury in mice. JCI Insight 7, e151869 10.1172/jci.insight.151869
22. Canessa CM, Merillat AM and Rossier BC (1994) Membrane topology of the epithelial sodium channel in intact cells. Am. J. Physiol 267, C1682–C1690 10.1152/ajpcell.1994.267.6.C1682 [PubMed: 7810611]
23. Mueller GM, Maarouf AB, Kinlough CL, Sheng N, Kashlan OB, Okumura S. et al. (2010) Cys palmitoylation of the beta subunit modulates gating of the epithelial sodium channel. J. Biol. Chem 285, 30453–30462 10.1074/jbc.M110.151845 [PubMed: 20663869]
24. Valentijn JA, Fyfe GK and Canessa CM (1998) Biosynthesis and processing of epithelial sodium channels in Xenopus oocytes. J. Biol. Chem 273, 30344–30351 10.1074/jbc.273.46.30344 [PubMed: 9804797]
25. Weisz OA, Wang JM, Edinger RS and Johnson JP (2000) Non-coordinate regulation of endogenous epithelial sodium channel (ENaC) subunit expression at the apical membrane of A6 cells in response to various transporting conditions. J. Biol. Chem 275, 39886–39893 10.1074/jbc.M003822200 [PubMed: 10978318]
26. Snyder PM, McDonald FJ, Stokes JB and Welsh MJ (1994) Membrane topology of the amiloride-sensitive epithelial sodium channel. J. Biol. Chem 269, 24379–24383 10.1016/S0021-9258(19)51094-8 [PubMed: 7929098]
27. Asher C, Wald H, Rossier BC and Garty H. (1996) Aldosterone-induced increase in the abundance of Na^+ channel subunits. Am. J. Physiol 271, C605–C611 10.1152/ajpcell.1996.271.2.C605 [PubMed: 8770001]
28. Masilamani S, Kim GH, Mitchell C, Wade JB and Knepper MA (1999) Aldosterone-mediated regulation of ENaC alpha, beta, and gamma subunit proteins in rat kidney. J. Clin. Invest 104, R19–R23 10.1172/JCI7840 [PubMed: 10510339]
29. Buck TM and Brodsky JL (2018) Epithelial sodium channel biogenesis and quality control in the early secretory pathway. Curr. Opin. Nephrol. Hypertens 27, 364–372 10.1097/MNH.0000000000000438 [PubMed: 29916852]
30. Buck TM., Jordahl AS., Yates ME., Preston GM., Cook E., Kleyman TR. et al. . (2017) Interactions between intersubunit transmembrane domains regulate the chaperone-dependent degradation of an oligomeric membrane protein. Biochem. J 474, 357–376 10.1042/BCJ20160760 [PubMed: 27903760]
31. Guerriero CJ, Gomez YK, Daskivich GJ, Reutter KR, Augustine AA, Weiberth KF et al. (2019) Harmonizing experimental data with modeling to predict membrane protein insertion in yeast. Biophys. J 117, 668–678 10.1016/j.bpj.2019.07.013 [PubMed: 31399214]
32. Gonzales EB, Kawate T. and Gouaux E. (2009) Pore architecture and ion sites in acid-sensing ion channels and P2X receptors. Nature 460, 599–604 10.1038/nature08218 [PubMed: 19641589]
33. Preston GM, Guerriero CJ, Metzger MB, Michaelis S. and Brodsky JL (2018) Substrate insolubility dictates Hsp104-dependent endoplasmic-reticulum-associated degradation. Mol. Cell 70, 242–53.e6 10.1016/j.molcel.2018.03.016 [PubMed: 29677492]

34. Guerriero CJ, Reutter KR, Augustine AA, Preston GM, Weiberth KF, Mackie TD et al. (2017) Transmembrane helix hydrophobicity is an energetic barrier during the retrotranslocation of integral membrane ERAD substrates. Mol. Biol. Cell 28, 2076–2090 10.1091/mbc.e17-03-0184 [PubMed: 28539401]
35. Loayza D, Tam A, Schmidt WK and Michaelis S. (1998) Ste6p mutants defective in exit from the endoplasmic reticulum (ER) reveal aspects of an ER quality control pathway in Saccharomyces cerevisiae. Mol. Biol. Cell 9, 2767–2784 10.1091/mbc.9.10.2767 [PubMed: 9763443]
36. Thomas C. and Tampe R. (2020) Structural and mechanistic principles of ABC transporters. Annu. Rev. Biochem 89, 605–636 10.1146/annurev-biochem-011520-105201 [PubMed: 32569521]
37. Deshaies RJ and Schekman R. (1990) Structural and functional dissection of Sec62p, a membrane-bound component of the yeast endoplasmic reticulum protein import machinery. Mol. Cell. Biol 10, 6024–6035 10.1128/mcb.10.11.6024-6035.1990 [PubMed: 2233730]
38. Mayer TU, Braun T. and Jentsch S. (1998) Role of the proteasome in membrane extraction of a short-lived ER-transmembrane protein. EMBO J. 17, 3251–3257 10.1093/emboj/17.12.3251 [PubMed: 9628862]
39. Scott DC and Schekman R. (2008) Role of Sec61p in the ER-associated degradation of short-lived transmembrane proteins. J. Cell Biol 181, 1095–1105 10.1083/jcb.200804053 [PubMed: 18573918]
40. Watts SG, Crowder JJ, Coffey SZ and Rubenstein EM (2015) Growth-based determination and biochemical confirmation of genetic requirements for protein degradation in Saccharomyces cerevisiae. J. Vis. Exp, e52428 10.3791/52428
41. Rubenstein EM, Kreft SG, Greenblatt W, Swanson R. and Hochstrasser M. (2012) Aberrant substrate engagement of the ER translocon triggers degradation by the Hrd1 ubiquitin ligase. J. Cell Biol 197, 761–773 10.1083/jcb.201203061 [PubMed: 22689655]
42. Buck TM, Kolb AR, Boyd C, Kleyman TR and Brodsky JL (2010) The ER associated degradation of the epithelial sodium channel requires a unique complement of molecular chaperones. Mol. Biol. Cell 21, 1047–1058 10.1091/mbc.e09-11-0944 [PubMed: 20110346]
43. Harty C, Strahl S. and Romisch K. (2001) O-mannosylation protects mutant alpha-factor precursor from endoplasmic reticulum-associated degradation. Mol. Biol. Cell 12, 1093–1101 10.1091/mbc.12.4.1093 [PubMed: 11294909]
44. Biederer T, Volkwein C. and Sommer T. (1996) Degradation of subunits of the Sec61p complex, an integral component of the ER membrane, by the ubiquitin-proteasome pathway. EMBO J. 15, 2069–2076 10.1002/j.1460-2075.1996.tb00560.x [PubMed: 8641272]
45. Inoue T. and Tsai B. (2016) The Grp170 nucleotide exchange factor executes a key role during ERAD of cellular misfolded clients. Mol. Biol. Cell 27, 1650–1662 10.1091/mbc.E16-01-0033 [PubMed: 27030672]
46. Cunningham CN, He K, Arunagiri A, Paton AW, Paton JC, Arvan P. et al. (2017) Chaperone-driven degradation of a misfolded proinsulin mutant in parallel with restoration of wild-type insulin secretion. Diabetes 66, 741–753 10.2337/db16-1338 [PubMed: 28028074]
47. Bernasconi R, Galli C, Calanca V, Nakajima T. and Molinari M. (2010) Stringent requirement for HRD1, SEL1L, and OS-9/XTP3-B for disposal of ERAD-LS substrates. J. Cell Biol 188, 223–235 10.1083/jcb.200910042 [PubMed: 20100910]
48. Neal S, Jaeger PA, Duttke SH, Benner C, K Glass C, Ideker T. et al. (2018) The Dfm1 Derlin is required for ERAD retrotranslocation of integral membrane proteins. Mol. Cell 69, 306–20.e4 10.1016/j.molcel.2017.12.012 [PubMed: 29351849]
49. Wang L, Li J, Wang Q, Ge MX, Ji J, Liu D. et al. (2022) TMUB1 is an endoplasmic reticulum-resident escortase that promotes the p97-mediated extraction of membrane proteins for degradation. Mol. Cell 82, 3453–67.e14 10.1016/j.molcel.2022.07.006 [PubMed: 35961308]
50. Noreng S, Bharadwaj A, Posert R, Yoshioka C. and Baconguis I. (2018) Structure of the human epithelial sodium channel by cryo-electron microscopy. eLife 7, e39340 10.7554/eLife.39340
51. Beggah A, Mathews P, Beguin P. and Geering K. (1996) Degradation and endoplasmic reticulum retention of unassembled alpha- and beta-subunits of Na,K-ATPase correlate with interaction of BiP. J. Biol. Chem 271, 20895–20902 10.1074/jbc.271.34.20895 [PubMed: 8702846]

52. Beggah AT, Beguin P, Bamberg K. and Sachs G. (1999) Geering K. beta-subunit assembly is essential for the correct packing and the stable membrane insertion of the H,K-ATPase alpha-subunit. J. Biol. Chem 274, 8217–8223 10.1074/jbc.274.12.8217 [PubMed: 10075726]
53. Beguin P, Hasler U, Beggah A, Horisberger JD and Geering K. (1998) Membrane integration of Na,K-ATPase alpha-subunits and beta-subunit assembly. J. Biol. Chem 273, 24921–24931 10.1074/jbc.273.38.24921 [PubMed: 9733799]
54. Beguin P, Hasler U, Staub O. and Geering K. (2000) Endoplasmic reticulum quality control of oligomeric membrane proteins: topogenic determinants involved in the degradation of the unassembled Na,K-ATPase alpha subunit and in its stabilization by beta subunit assembly. Mol. Biol. Cell 11, 1657–1672 10.1091/mbc.11.5.1657 [PubMed: 10793142]
55. Sottas V. and Abriel H. (2016) Negative-dominance phenomenon with genetic variants of the cardiac sodium channel Nav1.5. Biochim. Biophys. Acta 1863, 1791–1798 10.1016/j.bbamcr.2016.02.013 [PubMed: 26907222]
56. Helenius A. and Aebi M. (2001) Intracellular functions of N-linked glycans. Science 291, 2364–2369 10.1126/science.291.5512.2364 [PubMed: 11269317]
57. Snyder PM, Cheng C, Prince LS, Rogers JC and Welsh MJ (1998) Electrophysiological and biochemical evidence that DEG/ENaC cation channels are composed of nine subunits. J. Biol. Chem 273, 681–684 10.1074/jbc.273.2.681 [PubMed: 9422716]
58. Prince LS and Welsh MJ (1999) Effect of subunit composition and liddle's syndrome mutations on biosynthesis of ENaC. Am. J. Physiol 276, C1346–C1351 10.1152/ajpcell.1999.276.6.C1346 [PubMed: 10362597]
59. Kashlan OB, Kinlough CL, Myerburg MM, Shi S, Chen J, Blobner BM et al. (2018) N-linked glycans are required on epithelial Na^+ channel subunits for maturation and surface expression. Am. J. Physiol. Renal Physiol 314, F483–FF92 10.1152/ajprenal.00195.2017 [PubMed: 29187368]
60. Kanehara K, Kawaguchi S. and Ng DT (2007) The EDEM and Yos9p families of lectin-like ERAD factors. Semin. Cell Dev. Biol 18, 743–750 10.1016/j.semcdb.2007.09.007 [PubMed: 17945519]
61. Ushioda R., Hoseki J. and Nagata K. (2013) Glycosylation-independent ERAD pathway serves as a backup system under ER stress. Mol. Biol. Cell 24, 3155–3163 10.1091/mbc.e13-03-0138 [PubMed: 23966469]
62. Vasic V, Denkert N, Schmidt CC, Riedel D, Stein A. and Meinecke M. (2020) Hrd1 forms the retrotranslocation pore regulated by auto-ubiquitination and binding of misfolded proteins. Nat. Cell Biol 22, 274–281 10.1038/s41556-020-0473-4 [PubMed: 32094691]
63. Carvalho P, Stanley AM and Rapoport TA (2010) Retrotranslocation of a misfolded luminal ER protein by the ubiquitin-ligase Hrd1p. Cell 143, 579–591 10.1016/j.cell.2010.10.028 [PubMed: 21074049]
64. Stein A, Ruggiano A, Carvalho P. and Rapoport TA (2014) Key steps in ERAD of luminal ER proteins reconstituted with purified components. Cell 158, 1375–1388 10.1016/j.cell.2014.07.050 [PubMed: 25215493]
65. Baldridge RD and Rapoport TA (2016) Autoubiquitination of the Hrd1 ligase triggers protein retrotranslocation in ERAD. Cell 166, 394–407 10.1016/j.cell.2016.05.048 [PubMed: 27321670]
66. Peterson BG, Glaser ML, Rapoport TA and Baldridge RD (2019) Cycles of autoubiquitination and deubiquitination regulate the ERAD ubiquitin ligase Hrd1. eLife 8, e50903 10.7554/eLife.50903
67. Schafer A. and Wolf DH (2009) Sec61p is part of the endoplasmic reticulum-associated degradation machinery. EMBO J. 28, 2874–2884 10.1038/emboj.2009.231 [PubMed: 19696741]
68. Pilon M, Schekman R. and Romisch K. (1997) Sec61p mediates export of a misfolded secretory protein from the endoplasmic reticulum to the cytosol for degradation. EMBO J. 16, 4540–4548 10.1093/emboj/16.15.4540 [PubMed: 9303298]
69. Ng W, Sergeyenko T, Zeng N, Brown JD and Romisch K. (2007) Characterization of the proteasome interaction with the Sec61 channel in the endoplasmic reticulum. J. Cell Sci 120, 682–691 10.1242/jcs.03351 [PubMed: 17264153]
70. Mutchler SM, Kirabo A. and Kleyman TR (2021) Epithelial sodium channel and salt-sensitive hypertension. Hypertension 77, 759–767 10.1161/HYPERTENSIONAHA.120.14481 [PubMed: 33486988]

71. Bhalla V. and Hallows KR (2008) Mechanisms of ENaC regulation and clinical implications. J. Am. Soc. Nephrol 19, 1845–1854 10.1681/ASN.2008020225 [PubMed: 18753254]

72. Adams A, Gottschling DE, Kaiser CA and Stearns T. (1997) Methods in Yeast Genetics, A Cold Spring Harbor Laboratory Course Manual, Cold Spring Harbor, NY, USA

73. Mumberg D, Muller R. and Funk M. (1995) Yeast vectors for the controlled expression of heterologous proteins in different genetic backgrounds. Gene 156, 119–122 10.1016/0378-1119(95)00037-7 [PubMed: 7737504]

74. Zhang Y, Nijbroek G, Sullivan ML, McCracken AA, Watkins SC, Michaelis S. et al. (2001) Hsp70 molecular chaperone facilitates endoplasmic reticulum-associated protein degradation of cystic fibrosis transmembrane conductance regulator in yeast. Mol. Biol. Cell 12, 1303–1314 10.1091/mbc.12.5.1303 [PubMed: 11359923]

75. Huyer G, Piluek WF, Fansler Z, Kreft SG, Hochstrasser M, Brodsky JL et al. (2004) Distinct machinery is required in Saccharomyces cerevisiae for the endoplasmic reticulum-associated degradation of a multispanning membrane protein and a soluble luminal protein. J. Biol. Chem 279, 38369–38378 10.1074/jbc.M402468200 [PubMed: 15252059]

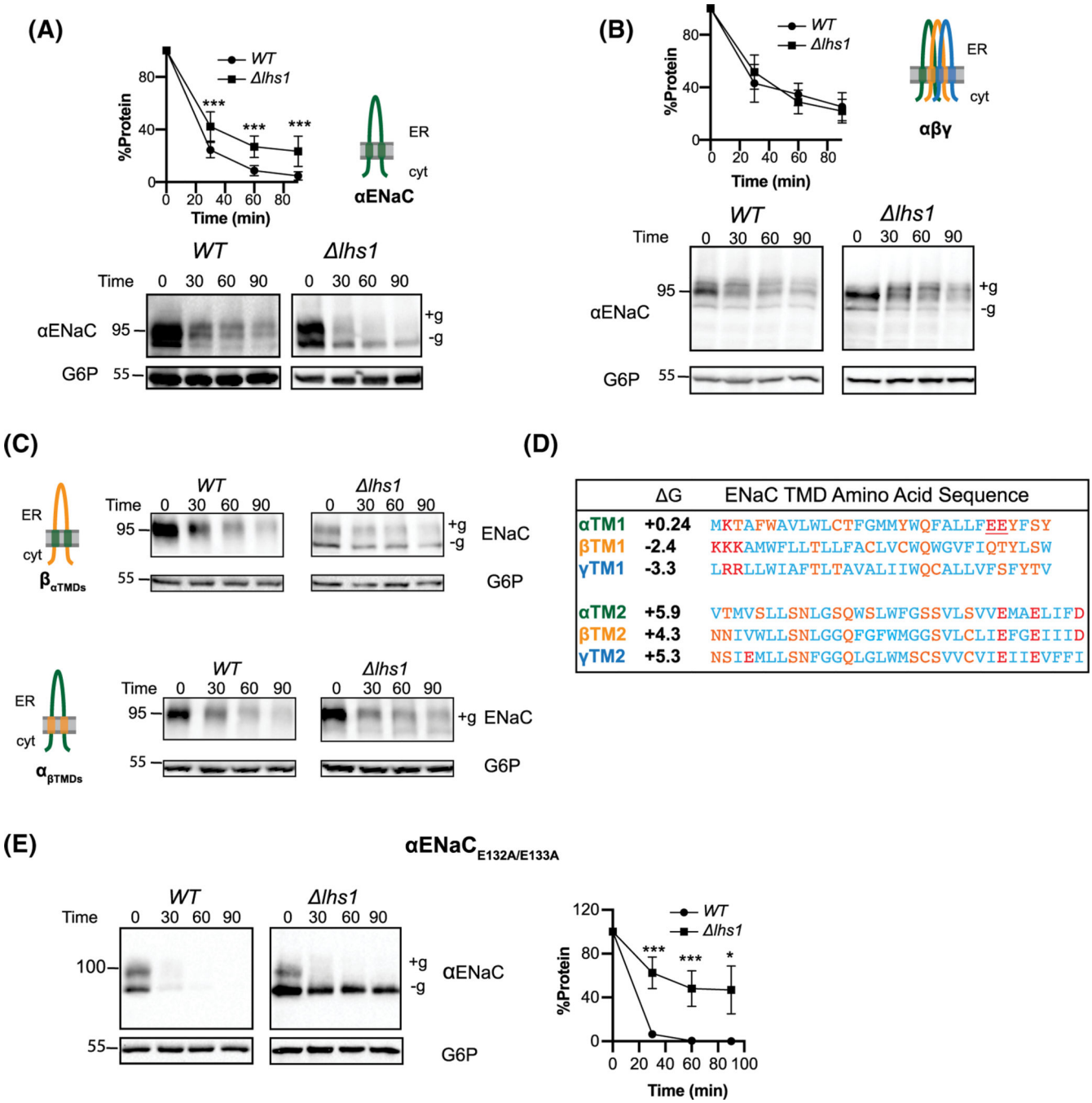

Figure 1. The Lhs1 dependence on αENaC biogenesis is based on transmembrane domain identity and is transferrable.

Cycloheximide chases were performed as described in Materials and Methods in either *WT* or *Δlhs1* yeast strain transformed with the indicated constructs: (**A**) αENaC, (**B**) αENaC with βγENaC, (**C**) $\beta ENaC_{\alpha TM1–2}$ or $\alpha ENaC_{\beta TM1–2}$, (**E**) $\alpha ENaC_{E133A/E134A}$. Protein lysates were prepared and immunoblotted with anti-HA (ENaC constructs) or anti-G6P (anti-glucose 6-phosphate dehydrogenase; Sigma) as a loading control. Data presented are representative images from $n \geq 4$ experiments, graphs represent mean ± SD; * $P < 0.05$,

*** $P < 0.001$. Glycosylated (+g) and unglycosylated (−g) protein species are noted. See Supplementary Figure S1 for quantitation of multiple replicates of the experiment shown in this panel (**D**) The apparent free energy for membrane insertion for each ENaC TMD (ΔG) was calculated as described in the text. Hydrophobic (blue), polar (orange), and charged (red) residues are indicated.

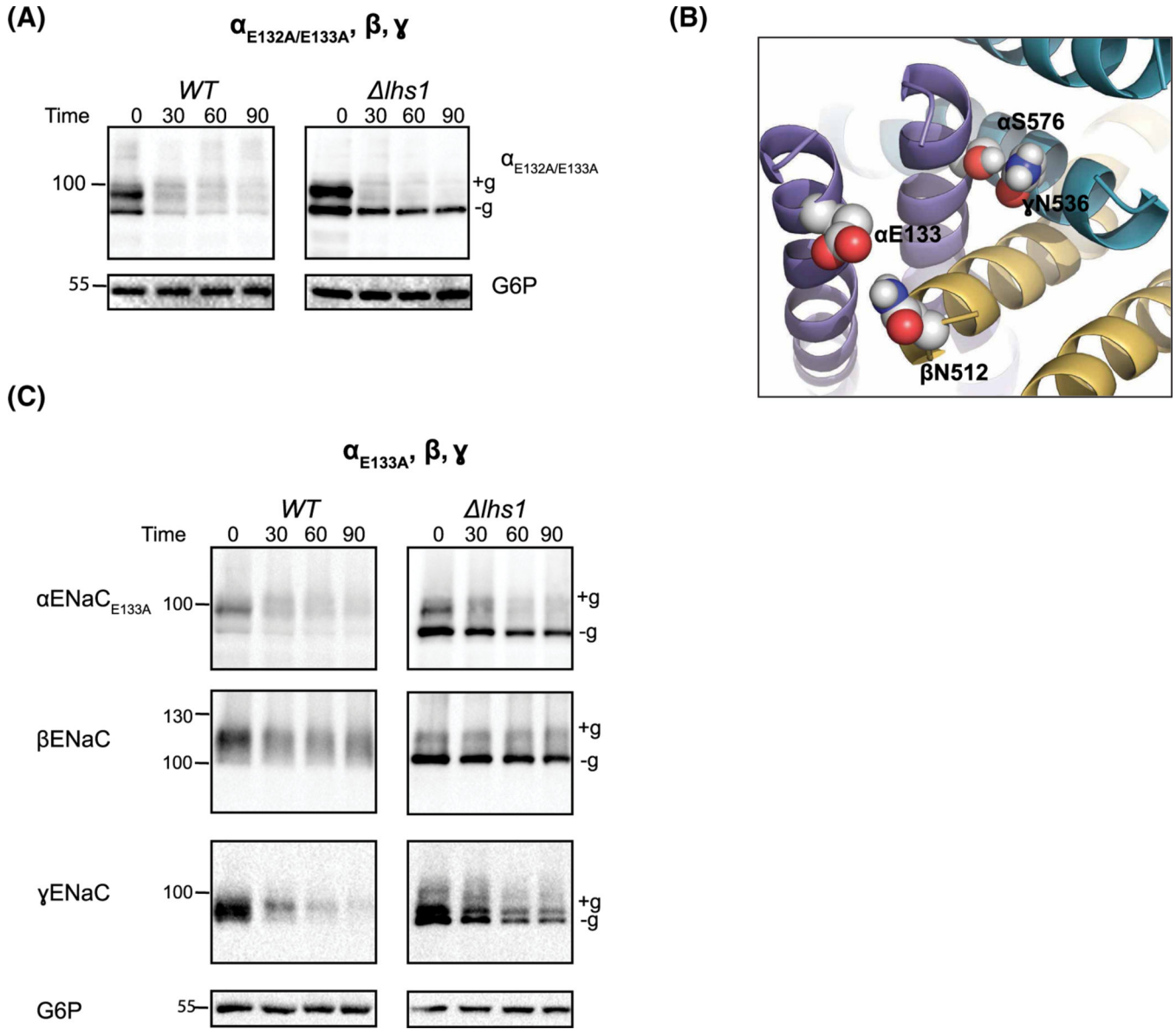

Figure 2. Disrupting the polar inter-subunit interactions between αENaC TMD1 and βENaC TMD2 maintain Lhs1-dependent degradation of all ENaC subunits.

(**A,C**) Cycloheximide chases were performed as described in Materials and Methods in *WT* or *Δlhs1* yeast strains transformed with three ENaC subunits as indicated above the western blots. Protein lysates were generated and immunoblotted with anti-HA antibody (αENaC constructs), anti-V5 antibody (γENaC), anti-myc (βENaC) or anti-G6P (anti-glucose 6-phosphate dehydrogenase; Sigma) as a loading control. Data presented are representative images from $n \geq 4$ experiments. Glycosylated (+g) and unglycosylated (−g) protein species are noted. (**B**) Structural model of the ENaC TMDs (αENaC purple, βENaC gold and γENaC teal). Space filling models indicate predicted, polar inter-subunit interactions.

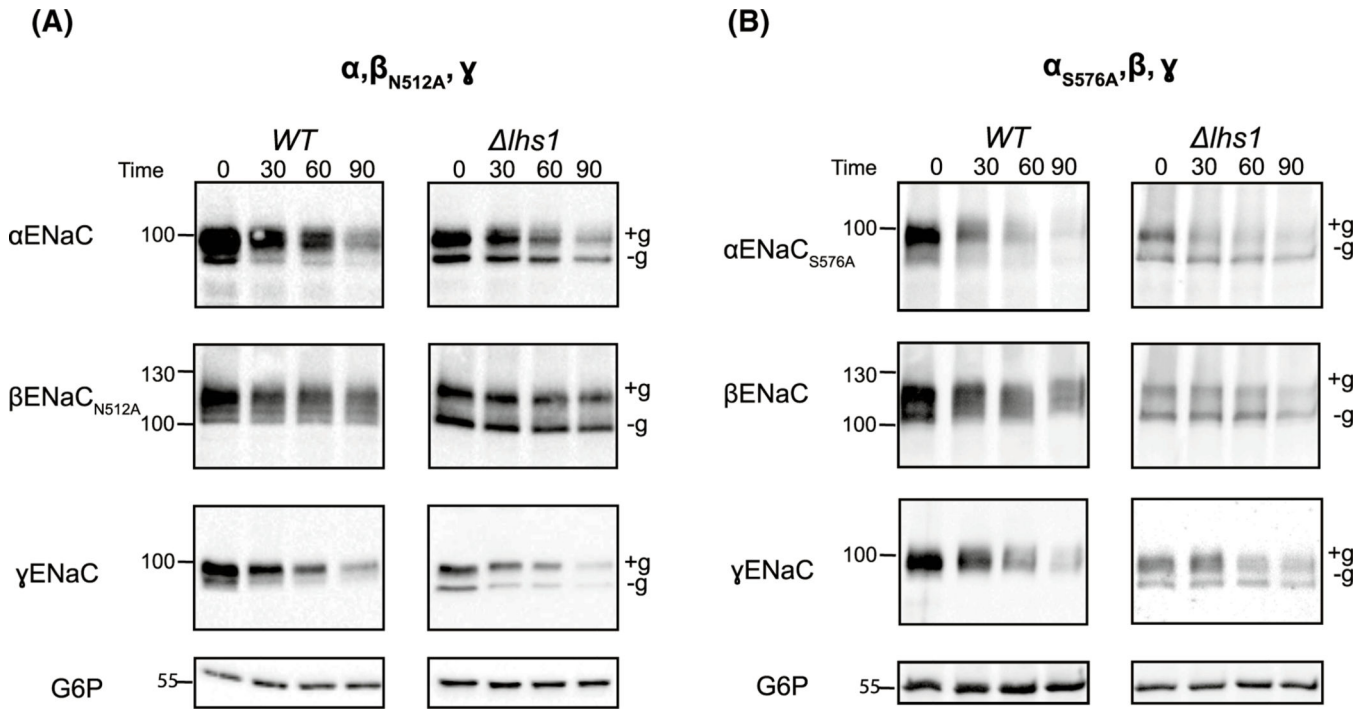

Figure 3. Disrupting the polar inter-subunit interactions between αENaC TMD2 and γENaC TMD2 maintain Lhs1-dependent degradation of ENaC subunits.

Cycloheximide chases were performed as described in Materials and Methods in *WT* or *Δlhs1* yeast strains transformed with (**A**) αENaC, βENaC$_{N512A}$ and γENaC, or (**B**) αENaC$_{S576A}$, βENaC and γENaC. Protein lysates were generated and immunoblotted with anti-HA antibody (αENaC constructs), anti-V5 antibody (γENaC), anti-myc (βENaC constructs), or anti-G6P (anti-glucose 6-phosphate dehydrogenase; Sigma) as a loading control. Data presented are representative images from $n \geq 4$ experiments. Glycosylated (+g) and unglycosylated (−g) protein species are noted.

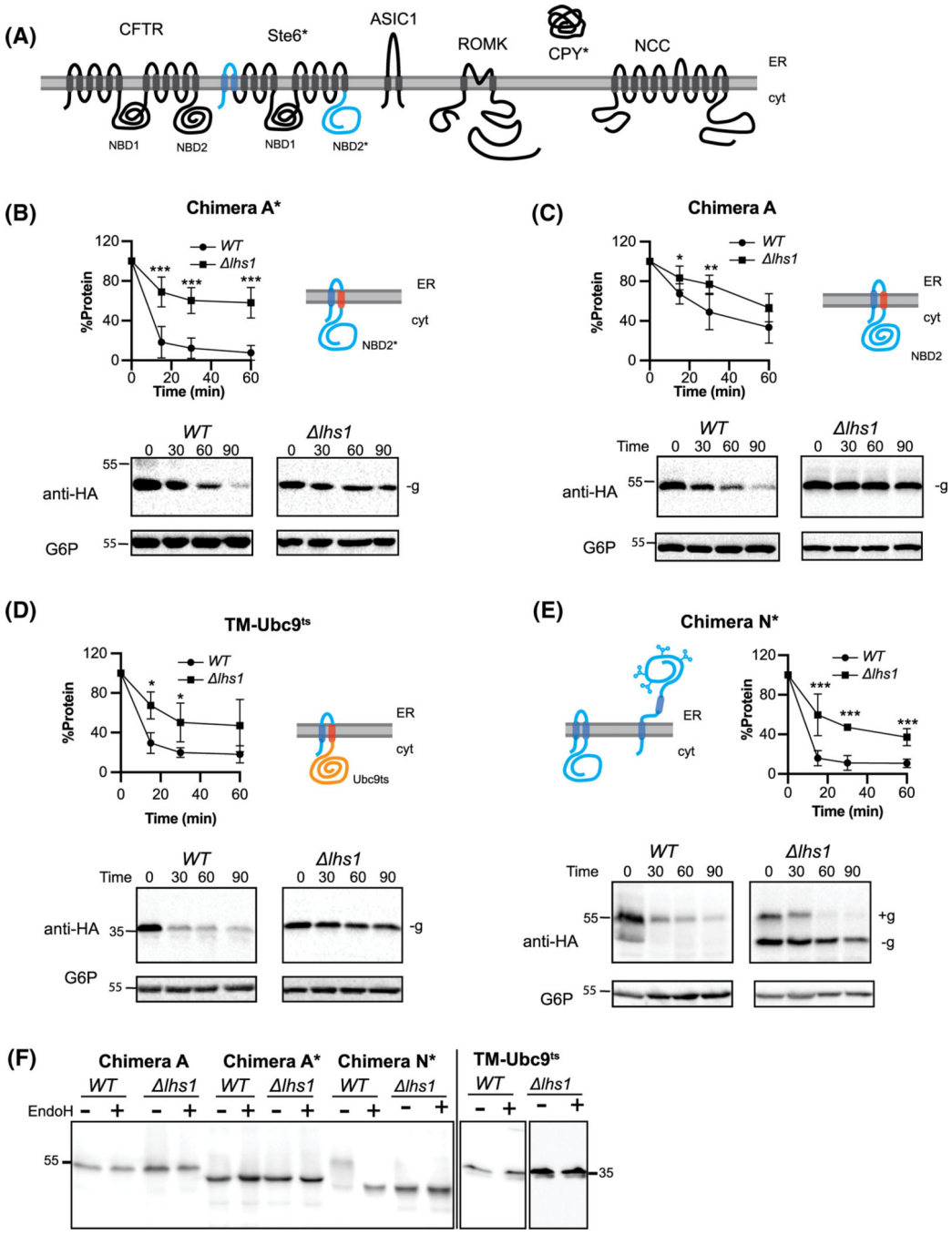

Figure 4. Dual-spanning model ERAD substrates exhibit Lhs1-dependent degradation.

(**A**) Shown are the diverse ERAD substrates for which the Lhs1 dependence was assessed. Topological models are depicted. (**B–E**) Cycloheximide chases were performed as described in Materials and Methods in *WT* or *Δlhs1* yeast strains transformed with the indicated constructs. Protein lysates were generated and immunoblotted with anti-HA antibody (Chimera series of constructs and TM-Ubc9^{ts}) or anti-G6P (anti-glucose 6-phosphate dehydrogenase; Sigma) as a loading control. Data presented are representative images from n ≥ 4 experiments, graphs present mean ± SD; * $P < 0.05$, ** $P < 0.01$, *** $P < 0.001$. (**F**)

Endo H digestion of the indicated protein lysates was performed as described in Materials and Methods. Protein lysates were immunoblotted with anti-HA antibody. Glycosylated (+g) and unglycosylated (−g) protein species are noted.

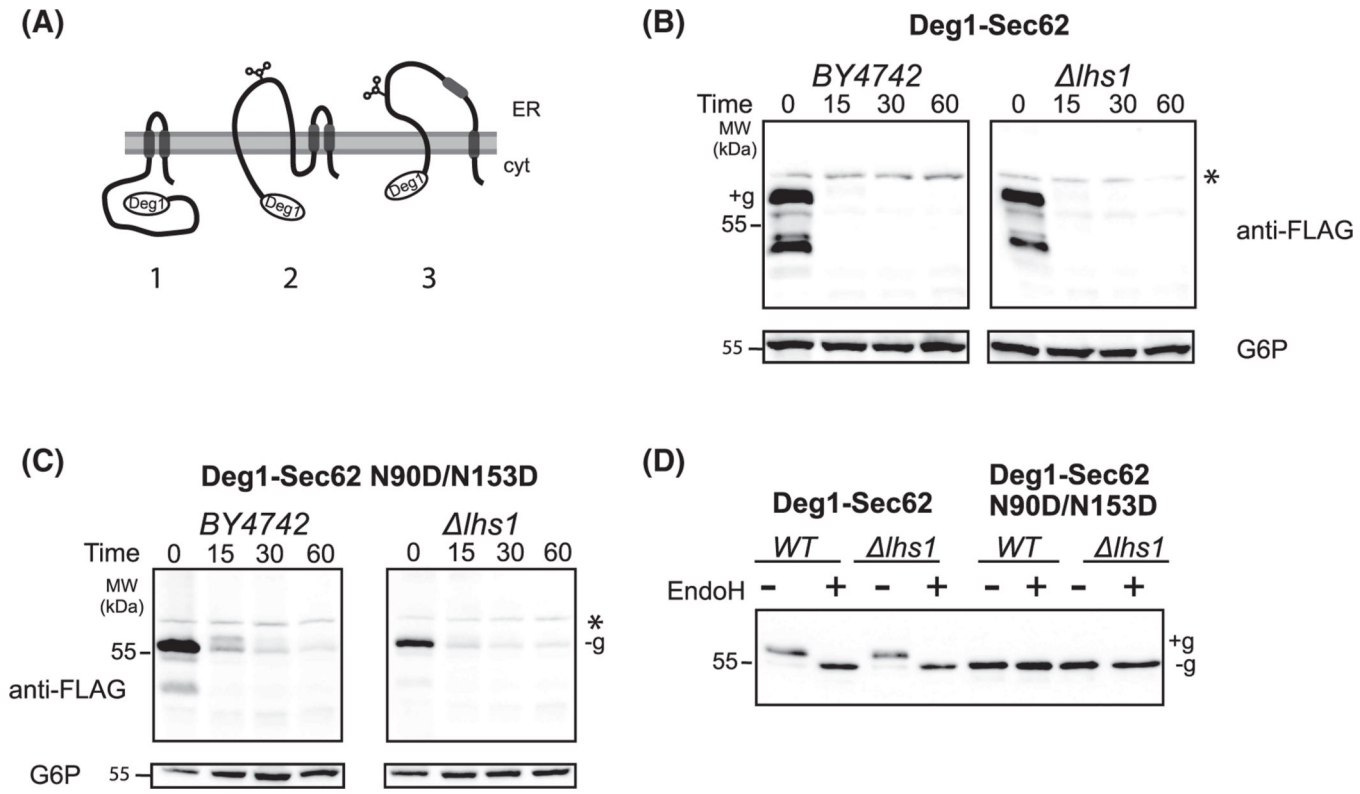

Figure 5. Degradation of the model ERAD substrate, Deg1–Sec62, is Lhs1 independent.

(**A**) Model of alternative topologies for Deg1–Sec62 proposed by Rubenstein et al. [41]. (**B,C**) Cycloheximide chases were performed as described in Materials and Methods in *WT* or *Δlhs1* yeast strains transformed with the indicated constructs. Protein lysates were generated and immunoblotted with anti-FLAG antibody (Deg1–Sec62 constructs) or anti-G6P (anti-glucose 6-phosphate dehydrogenase; Sigma) as a loading control. Data presented are representative images from $n \geq 4$ experiments. A darker exposure of Figure 5B is shown in Supplementary Figure S4B to illustrate the presence of the protein at later time-points. (**D**) Endo H digestion of the indicated protein lysates was performed as described in Materials and Methods. Glycosylated (+g) and unglycosylated (−g) protein species are noted and asterisk denotes a non-specific band.

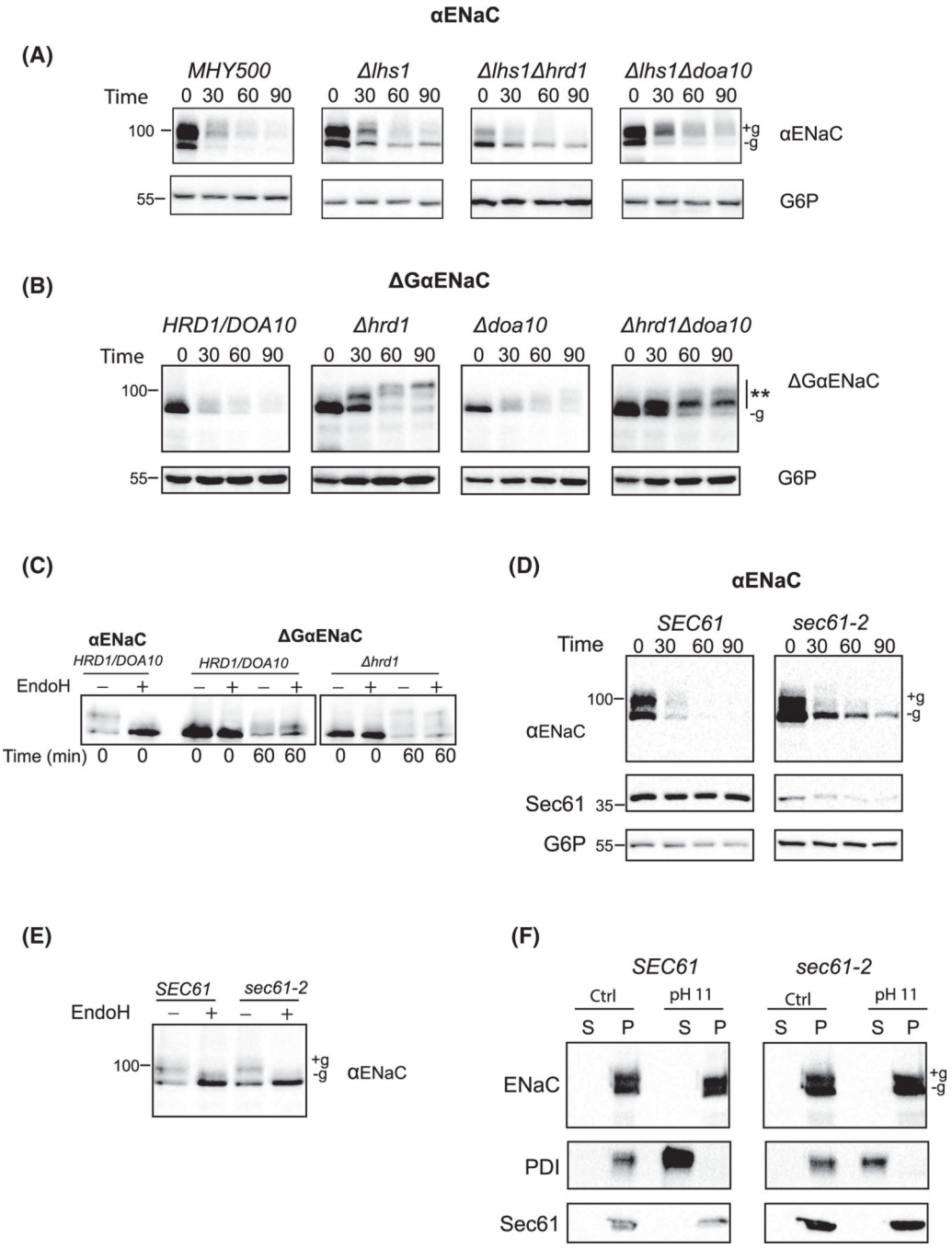

Figure 6. Lhs1 functions with the Hrd1/Sec62/Sec61 ERAD complex.

Cycloheximide chases were performed as described in Materials and Methods in the indicated yeast strains transformed with constructs to express either αENaC (**A,D**) or a form of αENaC lacking N-linked glycosylation sites (*ΔG*αENaC) (**B**). Protein lysates were generated and immunoblotted with anti-HA antibody (αENaC constructs) or anti-G6P (anti-glucose 6-phosphate dehydrogenase; Sigma) as a loading control. Protein lysates from cycloheximide chased performed in *HRD1/DOA10* and *Δhrd1* yeast strains [75] transformed with either αENaC or *ΔG*αENaC (**C**) or from *SEC61* and *sec61–2* strains

transformed with a construct to express αENaC (**E**) were digested with endoglycosidase H (EndoH) as described in Materials and Methods and immunoblotted with anti-HA antibody to detect ENaC. (**F**) Protein lysates from *SEC61* and *sec61–2* yeast strains transformed with a construct to express αENaC were subject to carbonate extraction as described in Materials and Methods. The resulting fractions were immunoblotted and probed with anti-HA antibody to detect αENaC, anti-Sec61 antibody and anti-PDI1 antibody. Glycosylated (+g) and unglycosylated (−g) protein species are noted. Data presented are representative images from $n \geq 4$ experiments.